05,07

Yttrium influence on magnetic properties and hyperfine interactions in multicomponent substitution alloys $(Dy_{1-x}Y_x)_{0.8}Sm_{0.2}Fe_2$

© Z.S. Umkhaeva[1], V.S. Rusakov[2], T.V. Gubaydulina[2], A.Yu. Karpenkov[3], I.S. Tereshina[2], N.Yu. Pankratov[2], I.M. Aliev[1]

[1] Kh. Ibragimov Complex Institute of the Russian Academy of Sciences, Grozny, Russia
[2] Moscow State University, Moscow, Russia
[3] Tver State University, Tver, Russia

E-mail: zargan.umhaeva@yandex.ru

Received October 6, 2023
Revised October 23, 2023
Accepted November 13, 2023

The paper presents the results of investigation of structure, magnetic properties and superfine interactions in multicomponent alloys based on rare-earth elements (R), Sm and their analogue Y of RFe_2 stoichiometry. To obtain new multicomponent alloys, a complex type of substitution in the rare-earth sublattice was used, namely, weakly magnetic samarium atoms at a fixed concentration of 20 at.% were first introduced into the dysprosium sublattice, followed by non-magnetic yttrium atoms at the values of the substitution parameter $x = 0$, 0.2, 0.4, 0.6, 0.8, 1.0. This type of substitution, first of all, leads to the competition of exchange interactions between magnetically active ions in a wide temperature region of their magnetic ordering. The competition also leads to a number of unique magnetic phase transformations in the resulting alloys, including the phenomenon of magnetic compensation of the rare-earth and 3d sublattice, as well as spin reorientation. The values of the main parameters of Mössbauer spectra on ^{57}Fe nuclei in $(Dy_{1-x}Y_x)_{0.8}Sm_{0.2}Fe_2$ alloys and their dependence on yttrium concentration at $T = 300$ K have been determined. The field dependences of magnetostriction in fields up to 12 kOe have been investigated.

Keywords: Laves phases, magnetization, Curie temperature, magnetic moment, Mössbauer effect, hyperfine interactions.

DOI: 10.21883/0000000000

1. Introduction

Intermetallic rare-earth metal (REM) compounds with iron-group elements (Fe, Co, Ni) have unique magnetic properties. These are primarily RFe_2 stoichiometry compounds known as Laves phases. two structural types of Laves phases with this stoichiometry occur: cubic Laves phase C15 and hexagonal Laves phase C14 [1–3].

To study the possibility of formation of new magnetic materials with pre-defined set of physical and chemical properties, multicomponent alloys based on the combination of various rare earth elements in a single sublattice. Whilst interatomic distances in substitution alloys may be varied and, thus, exchange interaction behavior may be also varied resulting in a particular type of magnetic ordering and in various kinds of phase transformation that depend essentially on the extent and type of substitution in REM or 3d sublattices. Hyperfine interactions that are usually investigated using the Mössbauer effect on ^{57}Fe nuclei are sensitive to the change of sign and type of exchange interactions. Comprehensive study of the structure, magnetic properties and hyperfine interactions in REM alloys with 3d transition metals is a crucial challenge.

In view of the above, the purpose of the study was to carry out detailed examination of the atomic and crystalline structure, magnetic properties and Mössbauer spectra parameters of dysprosium-based multicomponent alloys $(Dy_{1-x}Y_x)_{0.8}Sm_{0.2}Fe_2$, where x is the substitution parameter in a rare-earth sublattice. Selection of the study objects is based on the fact that, when atoms of heavy rare-earth Dy are first substituted with light rare earth Sm in fixed concentration and than with Y (non-magnetic equivalent of REM), competition of intersublattice exchange interactions will be observed in the system alloys in Dy−Fe and Sm−Fe pairs depending on the concentration of yttrium introduced into the rare-earth sublattice. Investigation of $(Dy_{1-x}Y_x)_{0.8}Sm_{0.2}Fe_2$ alloys will provide important data not only on the intersublattice exchange interaction R−Fe, but also on exchange interaction in the rare-earth sublattice, which shall surely have an effect on hyperfine interaction behavior of ^{57}Fe nuclei.

Practical significance of the study of rare-earth intermetallic compounds with the Laves phase structure is based on wide use of the compounds for various research and technology applications such as magnetostriction elements, gauges and fine movement sensors [4]. Therefore,

investigation of magnetostrictive strains of the produced $(Dy_{1-x}Y_x)_{0.8}Sm_{0.2}Fe_2$ alloys is also important.

2. Sampling and experiment procedure

To achieve the established target, we were the first to synthesize multicomponent alloys based on heavy rare-earth dysprosium $(Dy_{1-x}Y_x)_{0.8}Sm_{0.2}Fe_2$. Substitution parameter in these alloys is $x = 0$, 0.2, 0.4, 0.6, 0.8, 1.0.

The $(Dy_{1-x}Y_x)_{0.8}Sm_{0.2}Fe_2$ alloys were made by high-frequency induction melting in alundum crucible in high purity argon atmosphere at 70 kPa. Prior to heat treatment, 10–20 g ingot pieces were wrapped in nickel-iron foil and placed into a quartz tube that was first evacuated up to high vacuum, then filled with argon up to 70 kPa and sealed tightly. All samples were annealed for 40 h at 800°C, which was defined by the crystallization temperature of $SmFe_2$ phase (900°C). After annealing, the tube with samples was placed in water at about 0°C. The presence of inert gas, argon, in the tube facilitated rapid heat transmission in quenching compared with vacuum atmosphere and prevented alloy component evaporation at the annealing stage.

X-ray diffraction analysis (XPA) was performed for all samples using DRON-7 diffractometer in CuK_α-radiation ($\lambda = 0.1540598$ nm) at room temperature in the angle range $2\theta = 15-105°$. To determine structural properties, the diffraction patterns were analyzed using the spectrum fitting procedure. For this, each structural model was refined to convergence and the best results were chosen according to the coefficient of concordance and stability of refinement. The phase composition of the sample was analyzed by the Rietveld method.

Alloy magnetization was measured using a computer-aided vibrational magnetometer in stationary magnetic fields up to 1 T in the temperature range from 300 to 750 K.

Magnetostriction measurements were conducted by the strain-gauge method in magnetic field up to 12 kOe at $T = 300$ K. Foil strain gauges used herein were made from an alloy without significant galvanomagnetic effect. Gauge factor was equal to $S = 2.15$ throughout the temperature range. The gauges had a base length of 5 mm and resistance 120 Ω. For measurements, one gauge was attached to the sample and the other force-balance gauge was attached to a thin quartz plate that was pressed against the sample. Resistances of the primary and force-balance strain gauges differed by maximum 1%. Magnetostriction was measured on polycrystalline samples. longitudinal magnetostriction ($\lambda_\parallel$) and transverse magnetostriction ($\lambda_\perp$)were measured.

The Mössbauer spectra were measured in transmission geometry using MS-1104Em spectrometer in continuous acceleration mode. ^{57}Co gamma radiation source with ~ 20 mCu Rh matrix was used for the experiment. The spectrometer was calibrated at room temperature using α-Fe reference standard. Spectra were processed in SpectrRelax [5,6].

3. Experimental results and discussion

Multicomponent $(Dy_{1-x}Y_x)_{0.8}Sm_{0.2}Fe_2$ alloys were synthesized such as: $Dy_{0.8}Sm_{0.2}Fe_2$, $(Dy_{0.8}Y_{0.2})_{0.8}Sm_{0.2}Fe_2$, $(Dy_{0.6}Y_{0.4})_{0.8}Sm_{0.2}Fe_2$, $(Dy_{0.4}Y_{0.6})_{0.8}Sm_{0.2}Fe_2$, $(Dy_{0.2}Y_{0.8})_{0.8}Sm_{0.2}Fe_2$ and $Sm_{0.2}Y_{0.8}Fe_2$. Diffraction spectra of the above alloys were measured at room temperature (see Figure 1). According to XPA, all $(Dy_{1-x}Y_x)_{0.8}Sm_{0.2}Fe_2$ alloys are single-phase and have a cubic Laves phase C15 structure (space group $Fd\bar{3}m$). Crystalline structure features of RFe_2 stoichiometry compounds are well understood and described in many publications [1,3,6–8].

Calculation of lattice constants by diffraction peaks of the major phase has shown that the cubic lattice constant in $(Dy_{1-x}Y_x)_{0.8}Sm_{0.2}Fe_2$ compounds increases with yttrium concentration x growth from $a = 0.7338$ nm in $Dy_{0.8}Sm_{0.2}Fe_2$ ($x = 0$) to $a = 0.7368$ nm in $Y_{0.8}Sm_{0.2}Fe_2$ ($x = 1.0$) (Figure 2, *a*). It is known that cubic lattice cell constants in binary $DyFe_2$, $SmFe_2$ and YFe_2 compounds are equal to 0.7309, 0.7401 and 0.7363 nm, respectively [9], i. e. in the alloy with the maximum yttrium concentration, $Y_{0.8}Sm_{0.2}Fe_2$, the lattice constant is very close to that of binary YFe_2.

Thermomagnetic analysis method was used for this system alloys to measure the magnetic ordering temperature — Curie temperature (see Figure 2, *a*). It was found that the temperature decreases from $T_C = 587$ K for the $Dy_{0.8}Sm_{0.2}Fe_2$ ($x = 0$) alloy to $T_C = 501$ K for the $Dy_{0.8}Sm_{0.2}Fe_2$ ($x = 1$) alloy. At the specified temperature,

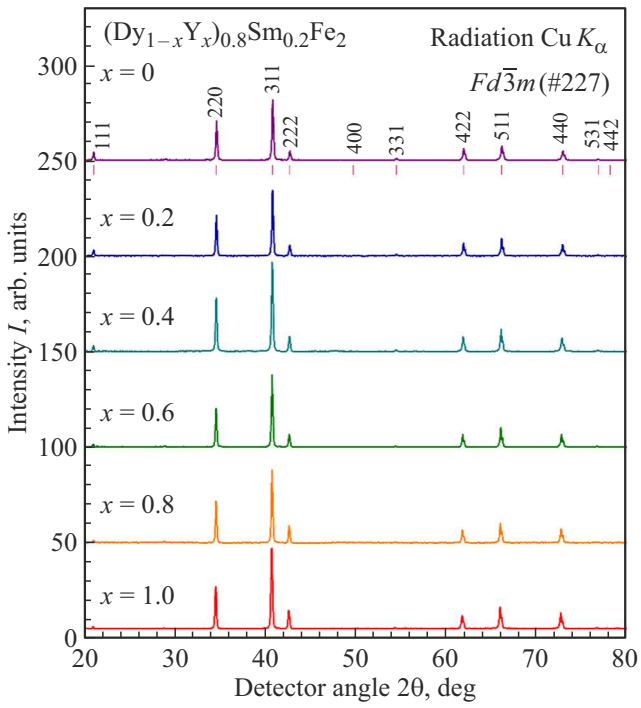

Figure 1. X-ray reflection spectra of the $(Dy_{1-x}Y_x)_{0.8}Sm_{0.2}Fe_2$ alloys at various values of substitution parameter x.

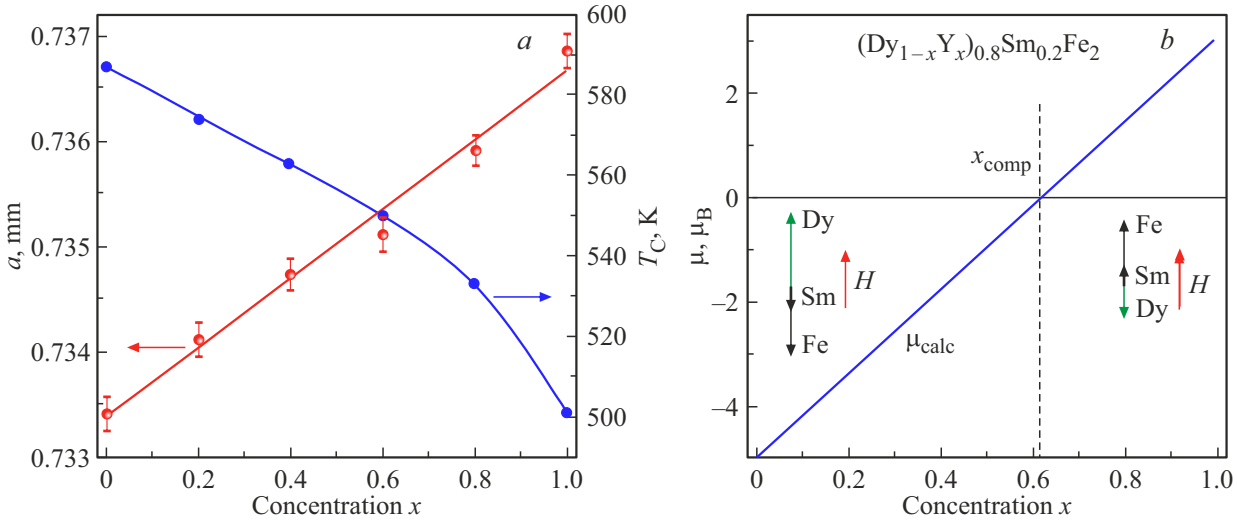

Figure 2. *a*) Crystal lattice constant and Curie temperature vs. substitution parameter x in the $(Dy_{1-x}Y_x)_{0.8}Sm_{0.2}Fe_2$ system. *b*) Design dependence of the full magnetic moment on yttrium concentration x at 0 K for the $(Dy_{1-x}Y_x)_{0.8}Sm_{0.2}Fe_2$alloys.

transition to paramagnetic state is observed in the alloys (this phase transformation is the „order–disorder“ transformation).

Our theoretical calculations within the collinear magnetic moment model have shown that the magnetic compensation point in the temperature region near the absolute zero in this system falls on the compound with yttrium concentration $x_{comp} = 0.62$ [10]. In our calculations, the full magnetic moment was calculated using the following equation

$$\mu_{calc} = 2\mu_{Fe} + 0.2\mu_{Sm} - 0.8(1-x)\mu_{Dy},$$

where $\mu_{Fe} = 1.45\,\mu_B$/at. is the magnetic moment of Fe determined from magnetization of YFe_2; $\mu_{Dy} = 10\,\mu_B$/at. (magnetic moments of Dy^{3+} are arranged antiparallel to the Fe sublattice moment); $\mu_{Sm} = 0.7\,\mu_B$/at. is the magnetic moment of Sm^{3+} oriented parallel to the Fe sublattice moment. Thus, the total magnetic moment of the compounds

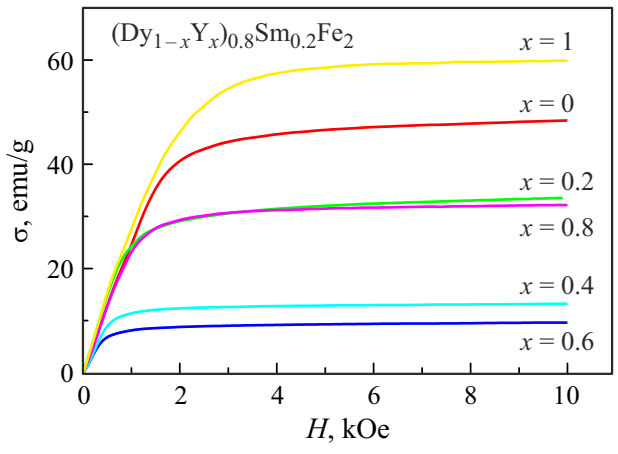

Figure 3. Specific magnetization of the $(Dy_{1-x}Y_x)_{0.8}Sm_{0.2}Fe_2$ alloys vs. external magnetic field at 300 K.

of interest depends linearly on the substitution parameter x (see Figure 2, *b*). Compound at which compensation is observed is called compensation compound. In our case, this is the $Dy_{0.3}Y_{0.5}Sm_{0.2}Fe_2$ compound.

Figure 3 shows specific magnetization curves of the $(Dy_{1-x}Y_x)_{0.8}Sm_{0.2}Fe_2$ alloys vs. external magnetic field at $T = 300$ K. The Figure shows that $\sigma(H)$ for all compounds are close to saturation in $H = 7$ kOe fields. Moreover, in $H < 3$ kOe fields, rapid growth of the specific magnetization is observed, and at $H > 3$ kOe, minor linear growth of $\sigma(H)$ curves is observed (paraprocess).

Figure 3 also shows that substitution of magnetoactive dysprosium atoms with non-magnetic yttrium atoms in accordance with the substitution parameter $x = 0.2$, 0.4, 0.6, 0.8, 1.0 results in considerable variation of specific magnetization values. From field magnetization measurements, saturation magnetizations for these compounds σ_s were defined by extrapolation of $\sigma(1/H)$ to the high field region.

It was found that saturation magnetization drops sharply from 47.8 emu/g at $x = 0$ to $\sigma_s = 9.26$ emu/g at $x = 0.6$. The the saturation magnetization increases again up to 59 emu/g at $x = 1$. Thus, in the yttrium concentration range $x = 0.6$, mutual magnetic compensation of magnetic moments of rare-earth and iron sublattices may be expected as it followed from theoretical calculations ($x_{comp} = 0.62$).

Figure 4 shows field dependences of magnetostriction of $(Dy_{1-x}Y_x)_{0.8}Sm_{0.2}Fe_2$ with various substitution parameters x. It should be noted that bulk (ω) and anisotropic (λ_a) magnetostrictions were calculated using the following equations

$$\omega = \lambda_{\parallel} + 2\lambda_{\perp}, \quad \lambda_a = \lambda_{\parallel} - \lambda_{\perp}.$$

In compounds with low yttrium concentration ($x \le 0.2$), longitudinal magnetostriction demonstrates complex alternating behavior of field dependence: it is negative in

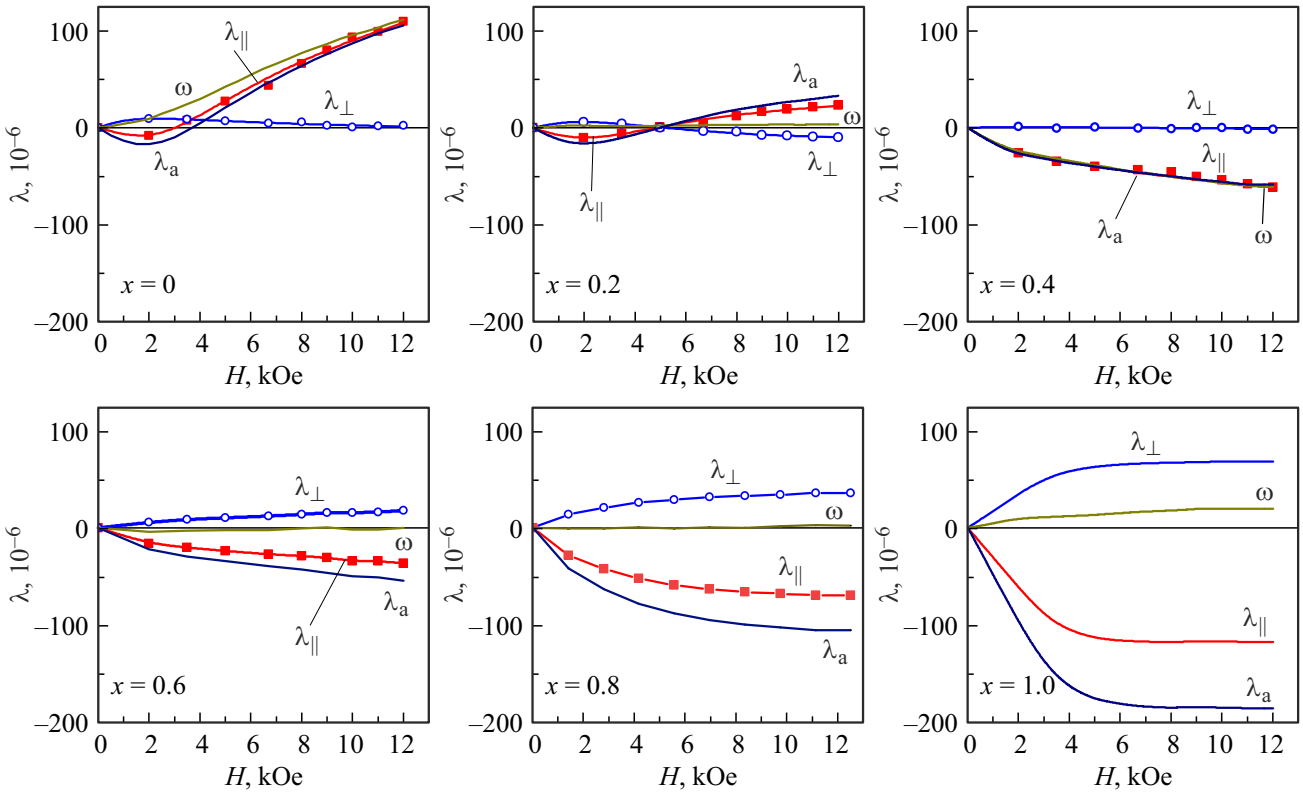

Figure 4. Dependences of the longitudinal, transverse, anisotropic and bulk magnetostriction on magnetic field strength at 300 K for $(Dy_{1-x}Y_x)_{0.8}Sm_{0.2}Fe_2$ compounds.

$H < 4$ kOe magnetic field, and with further field growth it changes sign and becomes positive. It should be noted that the longitudinal magnetostriction in compounds with$x \leq 0.4$ is near zero, therefore the main contribution to the bulk and anisotropic magnetostrictions in these compounds is provided by the longitudinal magnetostriction.

In the compound with $x \geq 0.4$, the longitudinal magnetostriction is negative in the magnetic field up to 12 kOe. At the same time, positive transverse magnetostriction occurs at $x > 0.5$. In $(Dy_{1-x}Y_x)_{0.8}Sm_{0.2}Fe_2$ with $x \leq 0.6$, the 12 kOe magnetic field is not sufficient to reach the saturation of magnetostriction curves $\lambda(H)$ due to high concentration of high-anisotropy Dy^{3+}. At the same time, in compounds with high yttrium concentration $(x \geq 0.8)$ and low dysprosium concentration, magnetostriction curves $\lambda(H)$ reach saturation in $H > 8$ kOe magnetic field. The longitudinal magnetostriction is negative and the transverse magnetostriction is positive. In all studied compounds, the bulk magnetostriction is low, excluding $Dy_{0.8}Sm_{0.2}Fe_2$.

Figure 5 shows concentration dependences of the longitudinal, transverse and anisotropic magnetostriction in the 12 kOe magnetic field at room temperature. Two linear segments may be found on all curves: the first — at $x \leq 0.4$ and the second — at $x \geq 0.6$.

Analysis of the value and sign of the longitudinal, transverse, bulk and anisotropic magnetostriction in compounds with low concentration of magnetoactive RE ions

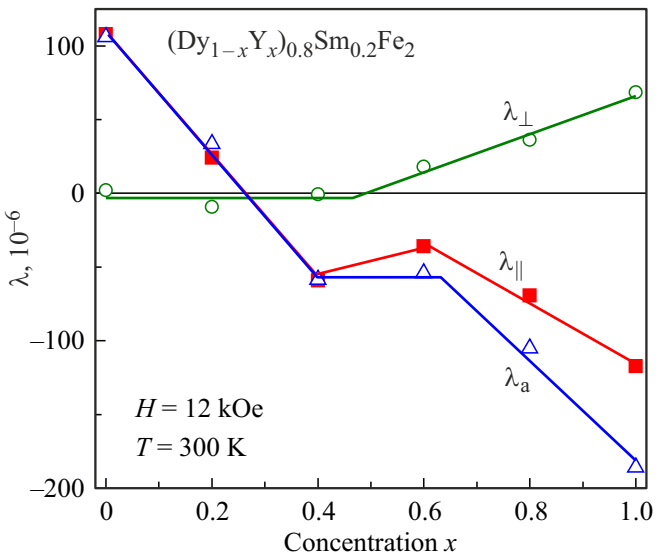

Figure 5. magnetostriction of $(Dy_{1-x}Y_x)_{0.8}Sm_{0.2}Fe_2$ alloys vs. yttrium concentration at 300 K.

(Dy and Sm) shows that the main contribution to the magnetostriction may be described under the single-ion model by the crystalline field mechanism and, therefore, magnetocrystalline interactions, in addition to exchange interactions, play an important role in these compounds.

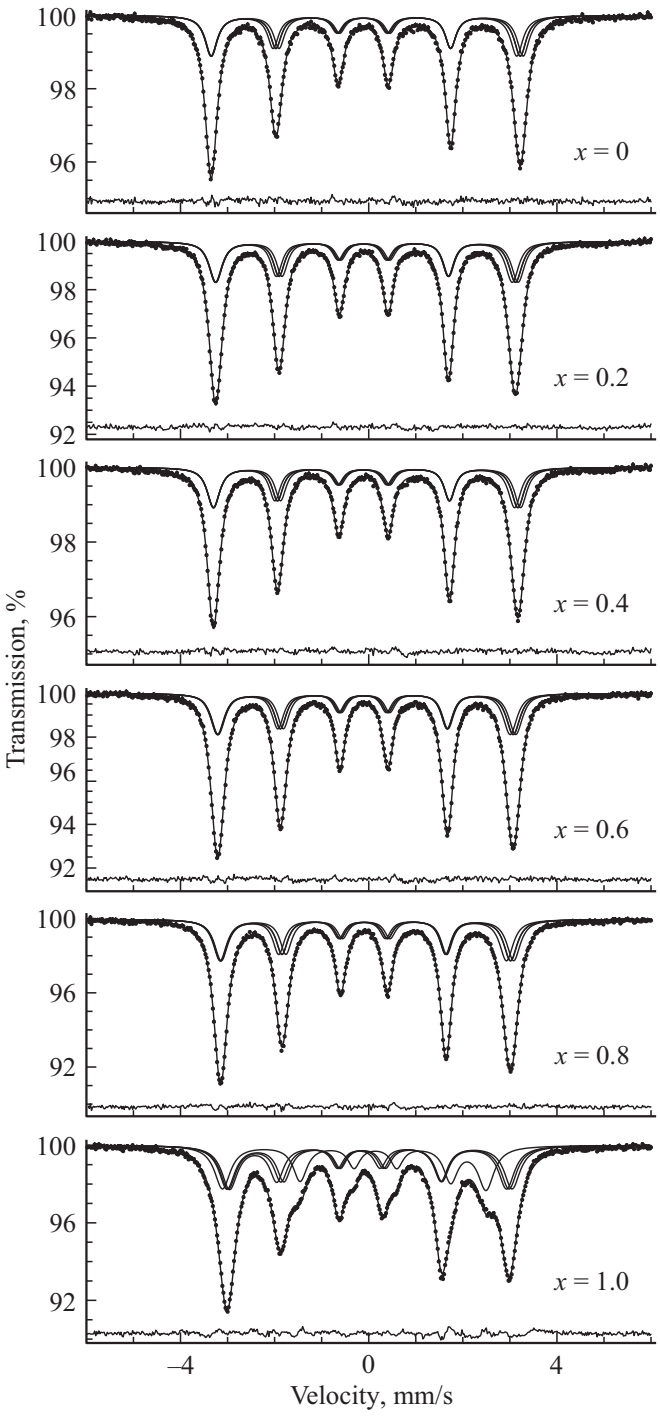

Figure 6. Model interpretation of spectra of ^{57}Fe nuclei in $(Dy_{1-x}Y_x)_{0.8}Sm_{0.2}Fe_2$.

It is known that in RFe_2 compounds and in substitution alloys on their basis, the magnetic moment on Fe atom is commonly believed to be almost constant within the experimental error and equal to $\mu_{Fe} = 1.45\,\mu_B$ like in the ferromagnetic YFe_2 compound [9]. Calculations of the magnetic moment on Fe atom conducted using the saturation magnetization σ_s deduced from experiments have shown that μ_{Fe} for alloys of the system under study is lower than this value and depends on the yttrium concentration in the REM sublattice. In the initial $Dy_{0.8}Sm_{0.2}Fe_2$ ($x = 0$), the experimental value of μ_{Fe} is equal to $1.16\,\mu_B$. With full substitution of Dy atoms by Y atoms ($Y_{0.8}Sm_{0.2}Fe_2$ alloy), $\mu_{Fe} = 1.12\,\mu_B$. Therefore, we have investigated the Mössbauer effect and found hyperfine magnetic fields indirectly associated with magnetic moments of Fe atoms [11].

The Mössbauer spectra on ^{57}Fe nuclei in $(Dy_{1-x}Y_x)_{0.8}Sm_{0.2}Fe_2$ alloy measured at room temperature (Figure 6) were analyzed within the tensor description of hyperfine magnetic interactions [12,13]. Spectra interpretation was conducted in SpectrRelax software [5,6] using the „Laves“ model described in detail in [14,15]. The model consists of four Zeeman sextets with hyperfine parameters whose interconnections consider the local magnetic inhomogeneity of Fe atom positions in RFe_2 type compounds with collinear magnetic and cubic (space group $Fd3m$) atomic structures and are based on relations (19)–(30) provided in [14]. The use of this model in minimization of χ^2, allows the optimum values of the physical quantities of interest to be found:

– shift of δ spectrum associated with the electron density in the nucleus region;

– quadrupole interaction constant e^2qQ between nuclei and environment creating inhomogeneous electric field on the nucleus;

– isotropic field H_{is} mainly based on the Fermi contact interaction with s-electrons localized on the nucleus and polarized conductivity electrons;

– anisotropic field H_{an}based on the magnetic dipole-dipole interaction with localized magnetic moments of the lattice atoms and polarized conductivity electrons;

– azimuthal φ and polar ϑ angles that define the easy axis (EA) orientation relative to the crystallographic axes.

Figure 6 shows that the „Laves“ model provides good description of the obtained ^{57}Fe nuclei spectra in the $(Dy_{1-x}Y_x)_{0.8}Sm_{0.2}Fe_2$ alloys.

Dependence of the shift of δ spectrum on the Y atom concentration obtained by means of model interpretation is shown in Figure 7. It is shown that the shift of δ spectrum, that is equal to the sum of the isomer shift due to the electron density in the nucleus region and of the temperature shift due to the dynamic nucleus properties, increases almost linearly with Y concentration.

The observed increase in the shift by 0.0071(7) mm/s with full substitution of Dy atoms by Y atoms (Figure 7) is primarily associated with an increase in the isomer shift due to the decrease in the electronic density on the nucleus with an increase in the lattice cell parameter (see Figure 2) and, therefore, in the interatomic distance, with substitution of Dy atoms by Y atoms.

Decreasing tendency of the quadrupole interaction constant (absolute value) e^2qQ observed in the $(Dy_{1-x}Y_x)_{0.8}Sm_{0.2}Fe_2$ alloys with atomic substitution of Dy by Y (Figure 8) is due to a decrease in the electric field gradient eq.

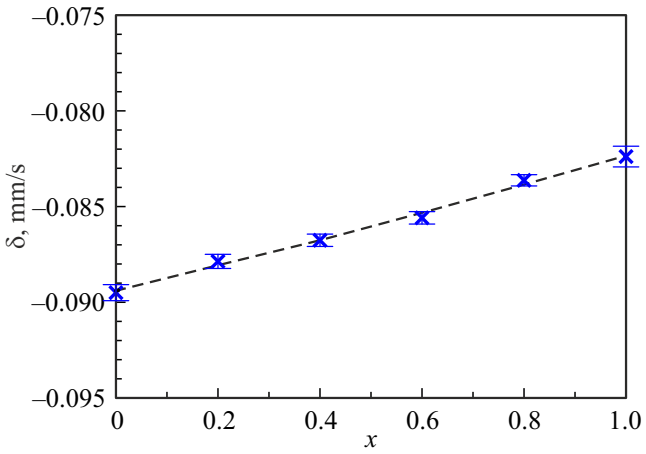

Figure 7. Shift of δ spectrum of ^{57}Fe nuclei vs. Y concentration in the $(Dy_{1-x}Y_x)_{0.8}Sm_{0.2}Fe_2$alloys.

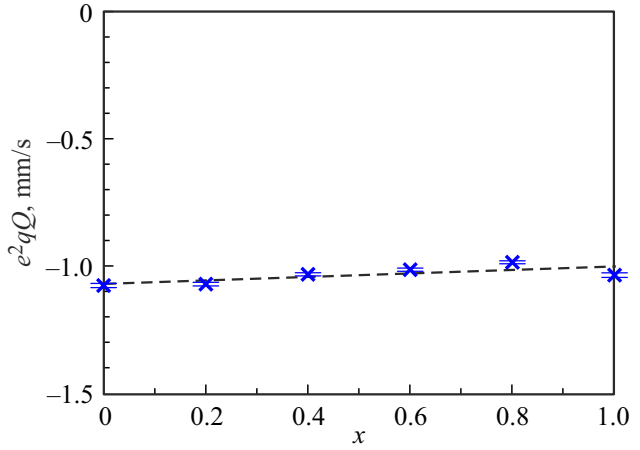

Figure 8. Quadrupole interaction constant e^2qQ of ^{57}Fe nuclei vs. Y concentration in the $(Dy_{1-x}Y_x)_{0.8}Sm_{0.2}Fe_2$alloys.

Such gradient decrease eq may be caused by a decrease in contributions to the inhomogeneous electric field on the nucleus due to localized charges of atom ion cores and polarized conductivity electrons with increase in interatomic distances that increase when Dy atoms are substituted by Y atoms.

When Dy atoms are substituted by Y atoms in the $(Dy_{1-x}Y_x)_{0.8}Sm_{0.2}Fe_2$ alloys, a decrease in the isotropic field by 19.94(6) kOe is observed in the ^{57}Fe nucleus region (Figure 9). According to the electronic structure calculation of the rare-earth Laves phases RFe_2 [16,17], 3d−5d-hybridization of electrons in ferromagnetic local spin interaction 4f−5d results in an increase in Fe ion spin (and magnetic moment) with an increase in the rare earth spin.

Such increase in the Fe ion spin, in turn, results in an increase in the main contribution of the Fermi contribution H_{Fermi} to the isotropic field. According to the theoretical calculations [18], the Fermi contribution to the isotropic field is proportional to the magnetic moment of 3d-shell of Fe atom. For crystalline and amorphous rare earth — Fe alloys, the coefficient of proportionality between the hyperfine magnetic field strength and magnetic moment of Fe atom equal to 145 kOe/$\mu_B$is commonly used [11,19]. Using the isotropic field data, magnetic moment of Fe atom in the $(Dy_{1-x}Y_x)_{0.8}Sm_{0.2}Fe_2$ alloys may be estimated at room temperature. For this, in Figure 9, besides the y axis for the isotropic field H_{is}, an axis for magnetic moment μ_{Fe} of Fe atoms is provided. μ_{Fe} values calculated from H_{is} were higher than those obtained by us from the magnetization investigations by an average of 11%.

For anisotropic hyperfine magnetic field H_{an}, dependence on Y concentration similar to that of the isotropic field H_{is} is observed: anisotropic field strength (absolute value) decreases by 5.3(2) kOe when Dy atoms are substituted by Y atoms (Figure 10). According to [20,21], contribution to the anisotropic field due to the conductivity electrons from the hybridized 3d−5d-band, polarized magnetic dipole

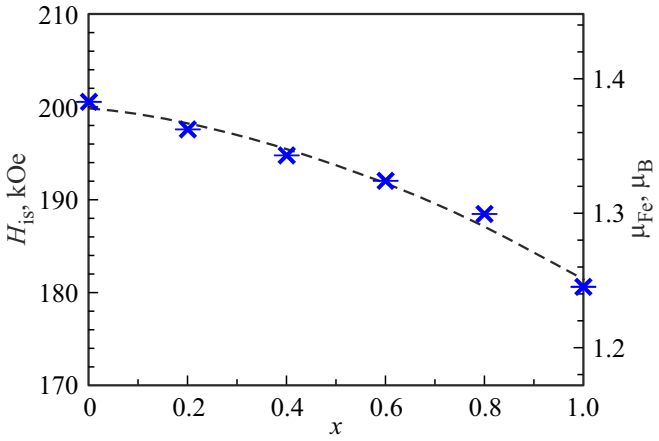

Figure 9. Isotropic field H_{is} on ^{57}Fe nuclei and magnetic moment μ_{Fe} of Fe atom vs. Y concentration in the $(Dy_{1-x}Y_x)_{0.8}Sm_{0.2}Fe_2$ alloys.

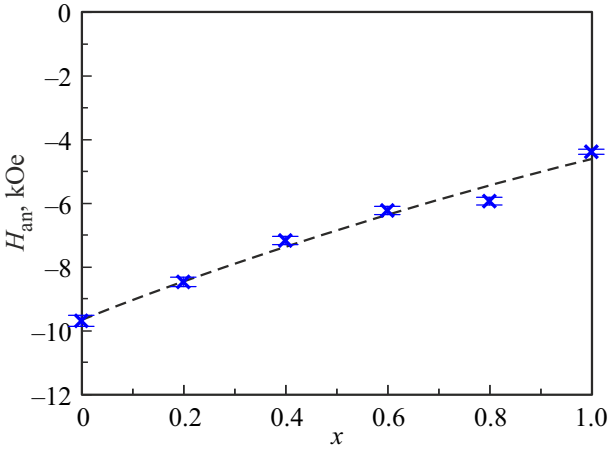

Figure 10. anisotropic field Han on ^{57} Fe nuclei vs. Y concentration in the $(Dy_{1-x}Y_x)_{0.8}Sm_{0.2}Fe_2$ alloys.

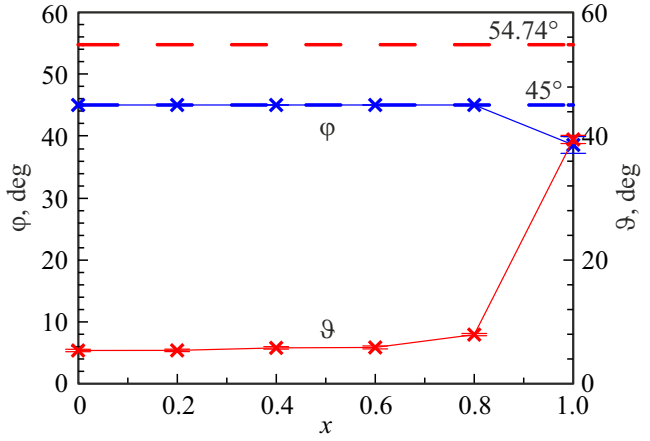

Figure 11. Azimuthal φ and polar ϑ angles that define the easy axis orientation relative to the crystallographic axes vs. Y concentration in the $(Dy_{1-x}Y_x)_{0.8}Sm_{0.2}Fe_2$ alloys.

field of the localized magnetic moments of lattice atoms, has the same sign as the dipole-dipole contribution. Both contributions to the anisotropic field, either dipole-dipole contribution from the localized magnetic moment of the lattice atoms or the contribution from he conductivity electrons, decrease with substitution of Dy atoms by Y atoms, because the mean magnetic moment of rare-earth atoms decreases and the interatomic distance increases.

Interpretation of spectra of the $(Dy_{1-x}Y_x)_{0.8}Sm_{0.2}Fe_2$ alloys in the „Laves" model allowed the EA orientation to be defined depending on the degree of Dy atom substitution by Y atoms (Figure 11). Spectra processing showed that up to $x = 0.8$, EA is in plane $(11\bar{0})$ (azimuthal angle $\varphi = 45°$) and deviates from axis (001) at a small angle ϑ that slightly increases from 5.4(2)° (at $x = 0$) to 7.9(2)° (at $x = 0.8$). With full substitution of Dy atoms by Y atoms, EA goes from plane $(1\bar{1}0)$ ($\varphi = 38.6(1.4)°$) and deviates from axis (001) towards the space diagonal ($\vartheta \cong 54.74°$) at $\vartheta = 39.4(7)°$. It is shown that for all $(Dy_{1-x}Y_x)_{0.8}Sm_{0.2}Fe_2$ alloys at room temperature, EA does not coincide with the crystallographic directions in the crystal. Such deviations of the EA orientation from the crystallographic directions at room temperature were observed in RFe_2 and earlier in [21–23].

4. Conclusion

The findings show that yttrium introduced into the rare-earth sublattice of $(Dy_{1-x}Y_x)_{0.8}Sm_{0.2}Fe_2$ rather actively effects the lattice constants and main magnetic properties of alloys. Growth of the substitution parameter x results in an increase in the crystalline lattice constant from $a = 0.7338$ nm in the initial $Dy_{0.8}Sm_{0.2}Fe_2$ ($x = 0$) alloy to $a = 0.7368$ nm in $Y_{0.8}Sm_{0.2}Fe_2$ ($x = 1.0$). In this case, interatomic distances vary in the rare-earth sublattice itself, which is accompanied by variation of not only intersublattice exchange interactions in Dy−Fe and Sm−Fe pairs, but also by variation of exchange interactions inside magnetic sublattices Dy−Dy, Dy−Sm, Sm−Sm and Fe−Fe. Competition between the listed types of interactions makes it possible to obtain compounds with full magnetic compensation of magnetization in a wide temperature range like in this system. It has been found that the magnetic compensation phenomenon is observed in the yttrium concentration region $x_{comp} = 0.6$, what coincided with $x_{comp} = 0.62$ theoretically calculated by us for this system.

The main magnetic properties were determined for the $(Dy_{1-x}Y_x)_{0.8}Sm_{0.2}Fe_2$ alloys. It has been established that when magnetoactive Dy atoms are substituted by non-magnetic Y atoms, the intersublattice exchange interaction Dy−Fe responsible for the Curie temperature decreased. Therefore, with growth of the substitution parameter x, the Curie temperature of the system alloys decreases from $T_C = 587$ K in $Dy_{0.8}Sm_{0.2}Fe_2$ to $T_C = 501$ K for $Y_{0.8}Sm_{0.2}Fe_2$. Magnetic moment values were defined per formula unit μ and Fe atom μ_{Fe} for each of the system alloys.

It is shown that spin reorientation in the concentration region $0.8 \leq x \leq 1$ and alternating behavior of longitudinal magnetostriction dependences (for compounds with $x = 0$ and 0.2) are observed in the system, as the most sensitive parameter to change of value and sign of exchange interactions.

Investigation of the Mössbauer effect made it possible to define some hyperfine structure parameters of the Mössbauer spectra of system alloys and to identify their behavior depending on Y concentration. It is shown that the isotropic field H_{is} gradually decreases with yttrium concentration growth in proportion to the drop of magnetic moment on Fe atom. In this case, a decrease in the anisotropic field H_{an} is observed in absolute value by 5.3 kOe. Isomeric shift δ and quadrupole interaction constants e^2qQ also depend on Y concentration.

Interpretation of the Mössbauer spectra of the $(Dy_{1-x}Y_x)_{0.8}Sm_{0.2}Fe_2$ alloys in the „Laves" model allowed the EA orientation to be defined depending on the degree of Dy atom substitution by Y atoms. It was found that for all $(Dy_{1-x}Y_x)_{0.8}Sm_{0.2}Fe_2$ alloys at room temperature, EA does not coincide with the crystallographic directions in the crystal.

Thus, the joint effect of the component concentration and external magnetic fields provide targeted influence on the exchange and magnetocrystalline interactions to forecast and obtain new magnetic-ordered alloys with optimum physical and chemical parameters for technical applications.

Funding

This study was supported by grant No. 22-22-00313 provided by the Russian Science Foundation, https://rscf.ru/project/22-22-00313/. The authors are grateful to Lomonosov Moscow State University for upgrading the research equipment used for the study. Melting and heat treatment of alloys, X-ray diffraction analysis and

measurements o field and temperature curves of specific magnetization were conducted using the equipment owned by the research and development laboratory of magnetic materials of the Center for the Collective Use of Scientific Equipment of Tver State University

Conflict of interest

The authors declare that they have no conflict of interest.

References

[1] A.S. Ilyushin. Vvedenie v srukturnuyu fiziku intermetallicheskikh soedineniy. MGU, M. (1984), 99 s. (in Russian).
[2] A.K. Kupriyanov, S.A. Nikitin, A.M. Sal'nikova, Z.S. Umkhaeva. FTT **31**, *11*, 297 (1989). (in Russian).
[3] K.A. Gschneidner Jr., L. Eyring. Physics and chemistry of rare earth elements. Nord-Holland Publishing Company, Amsterdam, N.Y., Oxford (1978). 336 p.
[4] K.P. Belov. Magnitostriktsionniye yavleniya i ikh tekhnicheskiye prilozheniya. Nauka, M., (1987), 159 s. (in Russian).
[5] M.E. Matsnev, V.S. Rusakov. AIP Conf. Proc. **1489**, 178 (2012).
[6] M.E. Matsnev, V.S. Rusakov. AIP Conf. Proc. **1622**, 40 (2014).
[7] T.A. Aleroeva, I.S. Tereshina, T.P. Kaminskaya, Z.S. Umkhaeva, A.V. Filimonov, P.Yu. Vanina, O.A. Alekseeva, A.S. Ilyushin. Phys. Solid State **61**, *12*, 2503 (2019).
[8] Z.S. Umkhaeva, I.S. Tereshina, N.Yu. Pankratov, I.M. Aliev, A.Yu. Karpenkov, Z.Sh. Gatsaev. Vestn. KNII RAN. Ser. Estestv. i tekh. nauki **2**, 101 (2022). (in Russian).
[9] K.N.R. Taylor. Intermetallic compounds of rare earth metals. University of Durham, UK (1971). Published: Adv. Phys. **20**, *87*, 551 (1971).
[10] Z.S. Umkhaeva, I.S. Tereshina, N.Yu. Pankratov, I.M. Aliev, F.S-A. Said-Akhmatova. Izv. ChGU **2**, *26*, 7 (2022). (in Russian).
[11] J. Chappert, J.M.D. Coey, D. Givord, A. Lienard, J.P. Rebouilliat. J. Phys. F **11**, *12*, 2727 (1981).
[12] V.I. Nikolaev, V.S. Rusakov, T.B. Solodchenkova. Izv. A. N. SSSR. Ser. fiz. **54**, *9*, 1681 (1990). (In Russian).
[13] B.C. Rusakov. Messbauerovskaya spektroskopiya lokalno neodnorodnykh sistem. IYaF NYaTs RK, Almaty (2000). 431 s. (in Russian).
[14] V.S. Rusakov, T.V. Gubaidulina, M.E. Matsnev, V.S. Pokatilov. Phys. Met. Metallogr. **120**, *4*, 339 (2019).
[15] M.E. Matsnev, V.S. Rusakov. Phys. Met. Metallogr. **124**, *3*, 279 (2019).
[16] M.S.S. Brooks, O. Eriksson, B. Johansson. J. Phys.: Condens. Matter **1**, *34*, 5861 (1989).
[17] M.S.S. Brooks, L. Nordstrom, B. Johansson. J. Appl. Phys. **69**, *8*, 5683 (1991).
[18] R.E. Watson, A.J. Freeman. Phys. Rev. **123**, *6*, 2027 (1961).
[19] K.H.J. Buschow, A.M. Van der Kraan. J. Magn. Magn. Mater. **22**, *3*, 220 (1981).
[20] U. Atzmony, M.P. Dariel. Phys. Rev. B **10**, *5*, 2060 (1974).
[21] P. Ray, S.K. Kulshreshtha. J. Physique **41**, *12*, 1487 (1980).
[22] C. Meyer, F. Hartmann-Boutron, Y. Gros, Y. Berthier, J.L. Buevoz. J. Physique **42**, *4*, 605 (1981).
[23] E.R. Bauminger, H.T. Savage. J. Appl. Phys. **52**, *3*, 2055 (1981).

Translated by E.Ilinskaya